


CONF-8305110-6

Los Alamos National Laboratory is operated by the University of California for the United States Department of Energy under contract W-7405-ENG-36

LA-UR--83-2113

DR63 015249

TITLE: PATTERN FORMATION BY SHOCK PROCESSES

AUTHOR(S): J. W.  M-G

SUBMITTED TO The Third Annual International Conference hosted by The Center for Nonlinear Studies, Los Alamos National Laboratory sponsored by Applied Mathematical Sciences Program US Department of Energy, 2-6 May 1983.

DISCLAIMER

This report was prepared as an account of work sponsored by an agency of the United States Government. Neither the United States Government nor any agency thereof, nor any of their employees, makes any warranty, express or implied, or assumes any legal liability or responsibility for the accuracy, completeness, or usefulness of any information, apparatus, product, or process disclosed, or represents that its use would not infringe privately owned rights. Reference herein to any specific commercial product, process, or service by trade name, trademark, manufacturer, or otherwise does not necessarily constitute or imply its endorsement, recommendation, or favoring by the United States Government or any agency thereof. The views and opinions of authors expressed herein do not necessarily state or reflect those of the United States Government or any agency thereof.

MASTER

By acceptance of this article the publisher recognizes that the U.S. Government retains a nonexclusive, royalty-free license to publish or reproduce the published form of this article, and to allow others to do so for U.S. Government purposes.

The Los Alamos National Laboratory requests that the publisher identify this article as work performed under the auspices of the U.S. Department of Energy.

Los Alamos Los Alamos National Laboratory Los Alamos, New Mexico 87545

PATTERN FORMATION BY SHOCK PROCESSES*

J. W. Shaner
Los Alamos National Laboratory

Abstract

Shock waves in condensed media often produce and leave behind periodic patterns and textures. These patterns have been observed both in real time and in post-mortum examination. In many cases the patterns can be related to analogous pattern-forming mechanisms in classical fluid dynamics, such as the Rayleigh-Taylor and Helmholtz instabilities. In other cases, the textures arise from peculiarities in the dynamic stress state immediately behind the leading edge of the shock wave.

Periodic waves in the interface between two shock welded metals have a close resemblance to the classical Helmholtz instability. From a practical point of view, these waves are crucial to the formation of a good bond.

Impulsive acceleration of an interface can result in the Meshkov instability, which forms patterns qualitatively similar to the Rayleigh-Taylor instability driven by continuous acceleration. However, the patterned stress state left behind after a shock crosses a perturbed interface can result in perturbation growth for shock propagation in either direction across the interface.

Even in homogeneous media, the non-hydrostatic component of the stress behind a shock can drive a pattern forming instability. Adiabatic shear banding has been proposed as a mechanism to explain both the patterns observed in shock-compressed and recovered metal samples and the apparent loss of macroscopic shear strength of shocked ceramics. New optical photographs of shocked quartz support this mechanism.

* Work supported by the United States Department of Energy.

Introduction

Shock waves in condensed media are usually associated with very destructive and chaotic explosions. However, even these destructive processes exhibit a wide variety of patterns formed directly behind the shock front. In some cases one can even recover, upon release of the shock pressure, pieces in which the shock-induced patterns are preserved.

Experiments over the past few decades have shown that a surprising degree of order and coherence persist behind a shock wave, at least until waves reflected from irregular boundaries seriously complicate the flow. For example, with the assumption that the stress behind a shock is hydrostatic, measurements of shock propagation have provided a good first approximation to much of our high pressure equilibrium equation of state data.¹ Furthermore, direct flash x-ray diffraction measurements have shown that even crystalline order is preserved behind a shock wave in solids, and that this order is coherent with respect to the unshocked crystal structure as well.²

In this paper I shall review and highlight three kinds of macroscopic patterns which occur in shock wave processes in condensed media. These patterns have in common that they evolve in a microsecond, or less, and that each is analogous to an instability in conventional fluid mechanics. The first is a wavy interface left behind when two metals are forced to collide at high velocity. These waves have features qualitatively like those found in the classical Kelvin-Helmholtz instability associated with shear flow in fluids. The second pattern I discuss is a periodic lamellar structure which has often been observed in metals and ceramics subjected to shock compression and recovered upon release. This phenomenon is related to a thermomechanical fluid instability usually referred to as adiabatic shear banding. The third pattern I discuss evolves after an initially planar shock wave passes a rippled interface separating two materials. This configuration is similar to the Rayleigh-Taylor instability problem. However, since for strong shocks even condensed media must be considered compressible, interesting non-linearities occur early in the growth of the initially perturbed interface.

Waves in Explosive Welding

In order to form good weld joints between metals, two essential conditions must be met. The metal surfaces must be uncontaminated (e.g. by oxide layers) and they must be brought into intimate contact. In fusion welding, the metals are actually melted and contaminations are allowed to float away from the joint region. In pressure welding, any surface layer of contaminants is broken up, allowing intimate contact, at elevated pressure, of the clean metals. Neither of these processes is very effective if the metals have widely different melting points or plastic flow strengths.

During World War I, ordinance specialists noticed that under certain conditions, bullets and shell fragments bonded to the metal target plates they hit. Although these may have been the first observations of explosive welding, the first published account did not appear until 1949.³ During the next two decades, a number of people began to exploit some of the unique features of explosive welding to make bonds between metals which would be impossible by other means.⁴ At the same time, carefully controlled experiments, where impact velocity and obliquity of collision were controlled, showed that ripples formed at the interface under the same conditions that favored good weld joints.^{5,6} These ripples are the subject of this section.

The ripples formed at the interface of two metals undergoing high velocity oblique impact were first studied systematically by Abrahamson.⁶ He used the configuration sketched in Fig. 1a. Flat nosed steel bullets were fired at thin metal targets inclined at an angle, θ , with respect to the front surface. In a coordinate system fixed at the point of contact, the target looks like an incident jet of velocity $V/\sin\theta$ and angle of incidence θ with respect to the plane of the bullet face. Abrahamson found that if $V/\sin\theta$ was less than the speed of sound in the target, or if it was supersonic but with θ greater than some critical value, waves were formed at the interface. If $V/\sin\theta$ was supersonic and θ was less than the critical value, no waves were formed.

For the subsonic case, simple conservation of momentum implies that the incident jet bifurcates into flows to the right and to the left along the bullet face in Fig. 1a. For supersonic flow with θ above a critical value, we also have conditions for a jet forming and flowing to the left away from the point of contact. For supersonic flow with smaller than critical obliquities, no such jet is formed, and the incident flow does not bifurcate. This behavior of supersonic flow is well known from the development of explosively driven shaped-charge jets.⁷

The correlation of a wavy interface with bifurcated flow and a jet emerging from the point of contact and flowing to the left in Fig. 1a suggests the Kelvin Helmholtz instability as a mechanism.^{8,9} In fact there must be large gradient in horizontal flow velocity at the planar bullet face. On the other hand, the large gradients along the bullet surface seriously complicate a quantitative analysis.

The configuration shown in Fig. 1b is now that most commonly used for welding and cladding, especially for very large pieces.¹⁰ In this configuration, V_p is the velocity given to the flyer plate by detonating explosive, while θ is the angle of impact. V_p can be varied by changing the type of explosive or the standoff between the flyer and the base plate. For steady flow, the point of contact moves with the detonation velocity ($V_c = V_p$), and V_p and θ are constants. This geometry can easily be transformed to that of Fig. 1a, and therefore, the jetting conditions are similar. For conditions favoring good weld joints, jets have actually been observed.¹¹

In the welding process, the function of the jet emerging from the contact point is easy to understand. The jet scrubs material from both the flyer and base plates allowing clean metal surfaces to come into contact at high pressures. For optimum welding, one needs a jetting configuration, and impact velocities high enough to cause metals to flow plastically but not so high that material at the interface melts. Rapid melting and resolidification seriously weakens the bond¹⁰.

The most detailed study of the waves on the welded interface was carried out by Bahrani, et.al.¹² In this study they found that as the wave amplitude grew, significant non-linearities appeared. By plating the steel base and flyer plates with copper and nickel, they were able to observe the effects of the jet and where in the interface profile remaining surface material wound up. Nickel from the flyer plate was concentrated in a vortex pattern behind the peaks of the waves, while copper from the base plate was moved ahead of the peak of the wave. Both copper and nickel were mixed in a vortex on the leading edge of the wave. The leading and trailing vortices are also asymmetric.

At the present time, the only theoretical and numerical analyses of these waves in weld joints have been qualitative or badly oversimplified. The analysis by Bahrani, et al.,¹² although in qualitative agreement with their experiments is not quantitative. The quantitative analyses, based on Kelvin-Helmholtz instability theory are successful at predicting wavelengths for the ripples, but these calculations do not address the vorticity and non-linear wave growth.^{8,9} Detailed calculations of the non-linear instability of parallel shear flows perhaps come closest to the experimental situation, except that we do not have a strictly parallel shear flow.¹³ Finally, the effects of interfacial energy, material strength, and compressibility have not been considered quantitatively. In conclusion we can say that we have enough empirical results to make good weld joints explosively. However, we do not yet have the analytical capability to predict the kinds of non-linearities which develop in the waves at the bonded interface.

Adiabatic Shear Banding

Another pattern often found in materials recovered after shock compression and release consists of roughly periodic lamellar structures along specific crystallographic planes. These features have been known for a long time in metals.¹⁴ Recently spatially periodic luminescence also been observed directly behind a shock front in quartz.¹⁵ Some crystallites in a polycrystalline sample show many such features, while others do not. The crystallite orientation with respect to the shock or release wave fronts

are obviously important. The connection between crystalline and stress tensor orientation is the key to the generation of these patterns.

In the simplest model for steady shock wave propagation in condensed media we consider the stress to be a simple scalar pressure. However, in even the earliest work on shocks in solids the authors realized that solids could support non-hydrostatic stresses.¹ Since the compression due to a shock wave is uniaxial in the direction of propagation, the natural choice of principle stresses are the longitudinal component, along the propagation direction, and the transverse components, assumed equal for isotropic materials. We expect that the longitudinal component will be greater than the transverse components, so long as the material can support shear stresses. With this stress configuration, the planes in which the shear stresses are maximum will lie at 45° to the longitudinal direction.

Under these conditions, as the shock strength is increased, the longitudinal component of the stress will increase, while the transverse component is determined solely by Poisson's ratio, until a point called the Hugoniot Elastic Limit is reached. At this point, the shear stresses in the planes at 45° to the propagation direction are the maximum the material can support, and stronger shocks will result in plastic deformation such that the resolved shear stresses remain bounded. This picture is the basis of the vonMises yield criteria often used in hydrodynamic flow calculations.

Within the framework of this simple model we would expect that as the shock strength increased, the longitudinal and transverse stresses would differ by an amount such that the maximum resolved shear stresses would be just enough to start plastic flow.

We show in Fig. 2 the various stress strain paths we expect if the material behaves hydrostatically or with a constant difference between longitudinal and transverse stress above the Hugoniot elastic limit.

For a number of years, however, we have suspected that the stress state behind a strong shock approaches hydrostatic (i.e. no stress deviators). This has been especially evident for brittle materials but more recent results suggest the same phenomenon for metals. In particular, by looking at the ability of shock compressed metals to support elastic recompression and decompression waves, Asay has shown that the intermediate stress-strain curve in Fig. 2 may be more appropriate for metals.¹⁶

A model developed by Grady shows the qualitative features resulting in the periodic structures.¹⁷ If an initially homogeneous material is allowed to evolve from initially uniform shear, it may develop a shear bonding instability under appropriate conditions. If, for example, the effective viscosity decreases with temperature, a local high temperature will cause concentration of the dissipative energy due to shear flow. As a result further temperature rises will further concentrate the shear flow.

For a two dimensional problem with material velocity, U , in the y direction and gradients only in the x direction, the flow equations are

$$\frac{\delta U}{\delta t} - \frac{1}{\rho_0} \frac{\delta \tau}{\delta x} = 0 \quad , \text{ and} \quad (1)$$

$$\frac{\delta T}{\delta t} - D \frac{\delta^2 T}{\delta x^2} = \frac{\tau}{\rho_0 C} \frac{\delta U}{\delta x} \quad (2)$$

In Eq. (1), ρ_0 is the density, and τ is the shear stress. In Eq. 2, D is the thermal diffusivity, which limits the local temperature rise, and C is the heat capacity. These equations must be completed by a third describing the relation of shear stress, velocity gradient and temperature. For example, Grady modeled the effective viscosity to give

$$\tau = [\eta_0 e^{-a(T-T_0)}] \frac{\delta U}{\delta x} . \quad (3)$$

By linearizing Eqs. 1-3 for small perturbations from a homogeneous state, and assuming solutions of the form $e^{\alpha t} e^{i\beta x}$, one obtains a curve for α vs $\beta=1/\lambda$ as shown in Fig. 3. The growth rate is limited for small wavelengths by the assumed thermal conduction.

The largest difficulty in applying this model quantitatively is establishing a realistic constitutive relation (3). With reasonable assumptions about the viscosity model, Hayes and Grady have shown that agreement can be obtained between the solution to Eqs. 1-3 and the observed lamellar structure in shocked aluminum with a wavelength of the order of 1-10 μm .¹⁸ The predicted growth rate at this wavelength is around 10^8 sec^{-1} , which is also appropriate for a shock process.

A much more detailed analysis, especially of Eq. (3) will be necessary before an understanding of the phenomenon of shear banding can be complete. For example, one would expect localized work hardening to play the same role of damping the instability as does thermal conduction. In the case of brittle solids one needs to include the surface energy generated by fractures, unless the confining pressure is so great that even brittle materials behave plastically. However, the adiabatic shear banding model does explain the apparent macroscopic hydrodynamic nature of solids under shock compression, and the varied patterns appearing during and upon recovery from shock waves.

Richtmyer-Meshkov (RM) Instability

When a shock wave passes an interface separating two fluids of differing density, an instability analogous to the classical Rayleigh-Taylor instability occurs. Since the shock accelerates the interface in the direction of propagation, any initial perturbations will grow if the acceleration is directed from the light fluid to the heavier fluid. However, there are several qualitative differences between the continuous acceleration and the impulsive acceleration cases.

In the original paper, Richtmyer solved numerically the hydrodynamic flow associated with the shock wave, or impulsive, acceleration of the interface between two fluids.¹⁹ The configuration is shown in Figure 4. An initial perturbation of the interface of the form $a_0 \cos kx$ was assumed. In the case of continuous acceleration, the time dependent amplitude is given by

$$\ddot{a} = kg(t) a(t) \left(\frac{\rho_2 - \rho_1}{\rho_2 + \rho_1} \right), \quad (4)$$

where $g(t)$ is the acceleration of the system and ρ_1 and ρ_2 are the densities.²⁰ If the acceleration is impulsive, as with a shock passing the interface, then

$$g(t) = U \delta(t), \quad (5)$$

where U is the material velocity jump across the shock. Integrating equation (4) then gives

$$\dot{a} = kUa_0 \left(\frac{\rho_2 - \rho_1}{\rho_2 + \rho_1} \right) \quad (6)$$

Although this expression is an oversimplification from several points of view, which will be discussed later, results derived from it agreed with Richtmyer's numerical calculations for γ -law gases, so long as he chose densities and an initial amplitude appropriate for the time just after the shock-interface interaction. For low amplitude shocks in ideal gases, the density ratio between singly shocked dense fluid (SF2 in Fig. 4) and doubly shocked light fluid (DSF1 in Fig. 4) is within a few percent of the initial density ratio. Therefore, the most sensitive parameters in Eq. (6), are a_0 , which can be compressed by a factor of two even with 0.1-0.2 MPa shocks in ideal gases, and the material velocity at the interface which may be less than half of that following the first shock in fluid 1. Uncertainty

in the choice of these parameters arises as a result of comparison of numerical results for compressible fluids with an analytical expression for incompressible fluids.

The simplified expression (6) does show a fundamental difference between the impulsive and constant acceleration cases. In the constant acceleration case, the perturbations grow only if the acceleration is directed from the light fluid to the heavy fluid. Otherwise the perturbation oscillates. On the other hand, equation (6) indicates that for an impulsive acceleration the perturbation of an interface grows no matter which direction the acceleration, or the direction of shock propagation, is. If a shock passes from a low density to a high density fluid the perturbation amplitude grows. If the shock propagates from a high density to a low density fluid, the amplitude passes through zero and grows with opposite phase.

Nine years after the Richtmyer work, Meshkov published experiments measuring interface perturbation growth with weak shocks (~ 0.1 MPa) in ideal gases (~ 0.1 MPa air, He, Freon, and CO_2).²¹ In these experiments he observed the linear growth of an initial perturbation when the shock passed from a light gas to a heavy gas. He also observed the reversal in phase and subsequent amplitude growth when the shock passed from the heavy to the light gas. These results, although in qualitative agreement with equation (6), showed growth rates only 0.5 times the predictions. The source of this discrepancy was presumed to be either an experimental problem associated with the film separating the gases, or the onset of non-linearity (Ka-1). No further experiments have been done to confirm these hypotheses.

An interesting feature found both in the numerical calculations and in a close examination of the experimental data is that even the initial growth of the perturbations is non-linear. The growth rate oscillates by 10-20% around the value predicted by Eq. (6). Richtmyer already identified this feature as due to the overstable nature of a rippled shock front in compressible fluids. In reference to Fig. 4, if the shock velocity in fluid 2 is slower than the incident shock in fluid 1, the transmitted shock will be rippled with an initial phase the same as that of the interface.

When such a shock wave propagates in a compressible fluid (i.e. finite sound velocity), pressure is concentrated behind the lagging part of the shock front by convergence. Therefore, the stress field immediately behind a rippled shock will have a coherent texture with respect to the ripples. In the subsequent flow, signals can propagate forward to the shock front, making the shock front non-steady, and backward to the original interface, superimposing another texture on this interface.

The overstable, or oscillatory nature of a rippled shock front has been measured directly in metals by Sakharov and Mineev.^{22,23} In these experiments, a rippled shock front was driven into metals at a stress level high enough that the metals behaved macroscopically like fluids. The phase of the ripples reversed before the shock front became planar indicating that the perturbation oscillates as it decays. This feature is a manifestation of the textured stress field left behind by non-planar shocks in a compressible medium.

Since the textured stress field behind a rippled shock depends on the nature of the ripples in the shock front, and since this texture can effect the initial non-linear growth of a perturbed interface, we have to look more closely at what variety of configurations of interface and stress waves are possible. The calculations of Richtmyer and Meshkov's experiments utilized only gamma-law ideal gases. For this restrictive equation-of-state, the density, ρ , is proportional to molecular weight, m . Similarly, the sound velocity, C , is proportional to $(T/m)^{1/2}$, where T is the temperature. In the limit of weak shocks, the shock impedance, $I = \rho C$, is then simply proportional to $m^{1/2}$. The shock impedances, shock velocities, and densities of the two fluids all play a role in the hydrodynamic evolution of the system.

The ideal gas equation-of-state allows only two of six qualitatively different configurations for the R-M instability. For example, we have already seen that if $\rho_2 > \rho_1$, the initial interface perturbation grows without change in phase. On the other hand, if $\rho_1 > \rho_2$, the initial perturbation changes phase before growing. Similarly, if $C_2 < C_1$, the transmitted shock wave is in phase with the initial interface perturbation.

Therefore, the initial regions of highest stress in the textured stress field behind the rippled transmitted shock will be near the part of the interface concave toward fluid 2. On the other hand if $C_2 > C_1$, the initial ripples in the transmitted shock are of opposite phase with respect to the interface perturbations, and the stress field texture induced by the rippled shock is the opposite from the $C_2 < C_1$ case. For ideal gases, if $\rho_2 > \rho_1$, then C_2 must be less than C_1 , and vice versa. However, it is easy to find pairs of materials with more general equations-of-state for which this role does not hold.

One further complexity concerns the relative shock impedance of the fluids. For the ideal gas equation of state, the denser fluid necessarily has the greater shock impedance. Therefore, if $\rho_2 > \rho_1$, then the wave reflected back into fluid 1 is a second shock, as shown in Fig. 4. Again it is easy to find pairs of materials for which $\rho_2 > \rho_1$, but $I_2 < I_1$. Then, although the interface perturbations still grow without change of phase, the reflected wave is a rarefaction. For a rippled rarefaction we should expect the stress field texture left behind to be roughly opposite in phase to that left by a shock. All of these cases are summarized in Table 1.

At this point, we should point out that even the complexities of Table 1 are not sufficient to cover all of the potential non-linearities in this originally simple hydrodynamic flow. Careful measurements by Sturtevant,²⁴ and Meshkov,²⁵ have demonstrated that the convergent parts of shock waves, even in ideal gases, undergo a complex time history, including the formation of Mach reflections, or three-shock intersection points. In the classic Mach reflection problem, we know that a slip line develops behind the triple shock interaction point, with a large flow velocity gradient across the slip line. In some cases this slip line is clearly unstable (Helmholtz instability), and persistent vortices can be left behind²⁶. Meshkov has also shown that similar complex wave interactions can develop in a rippled rarefaction wave.²⁷

Although we have listed the gross features which influence the non-linear growth of the RM instabilities in Table 1, the complexity of the details of flow associated with rippled waves may result in a much richer variety of possibilities. Fluid viscosity and interfacial tension will undoubtedly complicate the RM instability in fluids with weak shocks. We expect, for example, that if the interfacial energy density in the mixing region is comparable with the energy of compression by the shock wave, then surface tension will play a role in the subsequent flow. More careful measurements and reliable and detailed hydrocode calculations will be necessary to observe all of the non-linear phenomena associated with this instability.

We have outlined three qualitatively different kinds of non-linear instabilities resulting in pattern formation behind shock waves in condensed media. Each instability has an analog in more conventional fluid dynamics. A great deal of analytical work, particularly numerical calculations, will be necessary before we will be able to claim a detailed predictive capability for any of these pattern forming mechanisms. However, the strong analogies to better known fluid instabilities have given us significant insight into the processes at work even on the sub-microsecond time scale.

References

1. J. M. Walsh and R. H. Christian, Phys. Rev. 97, 1544 (1955).
2. Q. Johnson and A. C. Mitchell, Phys. Rev. Lett. 29, 1369 (1972).
3. L. R. Carl, Met. Prog. 46, 102 (1944).
4. R. Crossland and A. S. Bahrani, Contemp. Phys. 9 71 (1968).
5. W. A. Allen, J. M. Mapes, and W. G. Wilson, J. Appl. Phys. 25, 675 (1954).
6. G. R. Abrahamson, J. Appl. Mech. 83, 519 (1961).
7. J. M. Walsh, R. G. Shreffler, and F. J. Willig, J. Appl. Phys. 29, 349 (1953).
8. J. N. Hunt, Phil. Mag. 17, 669 (1968).
9. Yu. A. Gordopolov, A. N. Dremín, and A. N. Mikhailov, Fiz. Goreniya i. Vzryua 14, 77 (1978).
10. S. H. Carpenter and R. H. Whittman, Ann. Rev. of Matls. Sci. 5, 177 (1975).
11. O. R. Bergmann, G. R. Cowan, and A. H. Holtzman, Trans. Metal. Soc. AIME 236, 646 (1964).
12. A. S. Bahrani, T. J. Black, and B. Crossland, Proc. Royal Soc. A296, 123 (1967).
13. J. L. Robinson, J. Fluid Mech. 63, 723 (1974).

14. C. S. Smith, Trans. Metall. Soc. AIME (1958).
15. P. J. Brannon, C. H. Konrad, R. W. Morris, E. D. Jones, and J. Asay, Sandia Report SAND82-2469 (1983).
16. J. Asay, private communication.
17. D. Grady, J. Geophys. Res. 85, 913 (1980).
18. D. B. Hayes and D. E. Grady in Shock Waves in Condensed Matter - 1981, P412 AIP, New York 1982.
19. R. D. Richtmyer, Comm. on Pure and Appl. Math XIII, 297 (1960).
20. G. Taylor, Proc. Royal Soc. (London) A201 (1950).
21. E. E. Meshkov, Izv. ANSSSR. Mekh. Zhidkosti i Gaza 4, 151 (1960).
22. A. D. Sakharov, R. M. Zaidel', V. N. Mineev, and A. G. Oleinik, Soviet Physics - Dokl. 9, 1091 (1965).
23. V. N. Mineev and E. V. Savinov, Soviet Physics JETP 25, 411 (1967).
24. B. Sturtevant and V. A. Kulkarny, J. Fluid Mech. 73, 651 (1976).
25. E. E. Meshkov and V. N. Mokhov, Fiz Goreniya i Vzryun 18, 93 (1982).
26. R. E. Duff, Proc. Symposium in Appl. Math 13, 77 (1962).
27. B. A. Klopov and E. E. Meshkov, Fiz. Goreniya i. Vzryun 18, 96 (1982).

TABLE 1. POSSIBLE RM CONFIGURATIONS

<u>CASE</u>	<u>DENSITY</u>	<u>SOUND VELOCITY</u>	<u>IMPEDANCE</u>	<u>SHOCK</u>	<u>INTERFACE</u>	<u>REFLECTED WAVE</u>	<u>EXAMPLE</u>
1	$\rho_2 > \rho_1$	$c_2 > c_1$	$I_2 > I_1$	- ^b	+ ^a	S ^c	Cu/PMMA
2	$\rho_2 > \rho_1$	$c_2 < c_1$	$I_2 > I_1$	+	+	S	IDEAL GASES
3	$\rho_2 > \rho_1$	$c_2 < c_1$	$I_2 < I_1$	+	+	R ^d	Teflon/Be
4	$\rho_2 < \rho_1$	$c_2 > c_1$	$I_2 > I_1$	-	-	S	Be/Teflon
5	$\rho_2 < \rho_1$	$c_2 > c_1$	$I_2 < I_1$	-	-	R	IDEAL GASES
6	$\rho_2 < \rho_1$	$c_2 < c_1$	$I_2 < I_1$	+	-	R	PMMA/Cu

- a. In phase with original perturbation.
- b. Opposite phase with respect to original perturbation
- c. Shock wave.
- d. Rarefaction wave.

Figure Captions

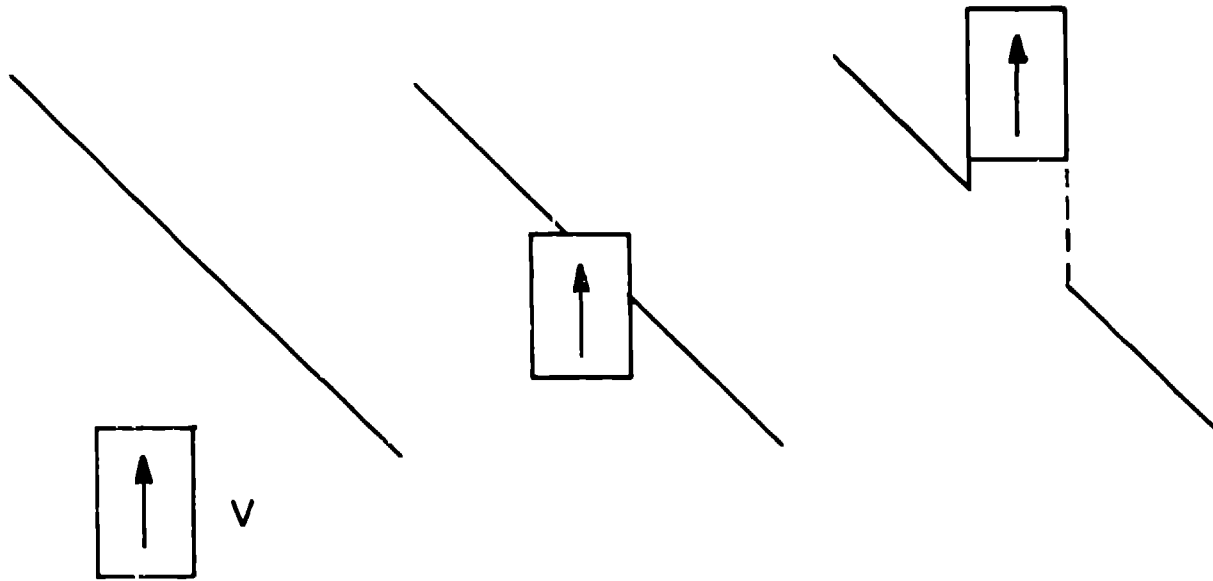
Fig. 1. A. A flat-nosed bullet, fired obliquely into a target plate can develop ripples in the bullet face.

B. The most useful configuration for explosive welding results in ripples at the weld joint.

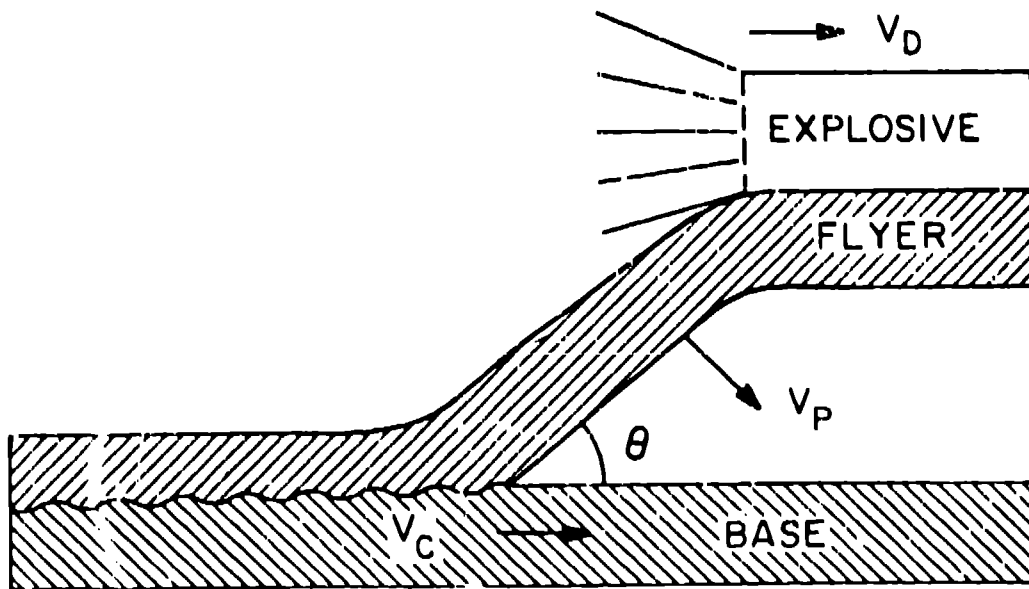
Fig. 2. Longitudinal stress vs strain for various compression processes. The Hugoniot represents a possible track for shock compression. τ_c represents the maximum stress deviator the material can support. If the stress behind a shock front had no tendency to approach a hydrostatic state, compression would be along the upper yield curve.

Fig. 3. Schematic of the solution to the linearized version of Eqs. 1-3. The growth rate for adiabatic shear bands is limited at large wavenumber by thermal conduction.

Fig. 4. Configuration for observing Richtmyer-Meshkov instabilities. On the left, a shock is incident from fluid 1 (F1). The shocked fluid is denoted SF1. On the right, after this shock has passed the fluid interface, the transmitted shock separates fluid 2 (F2) from the shocked fluid 2 (SF2). The reflected shock separates shocked fluid 1 (SF1) from the double shocked fluid (DSF1).



A. BULLET EXPERIMENT



B. EXPLOSIVE WELDING

Figure 1a and 1b.

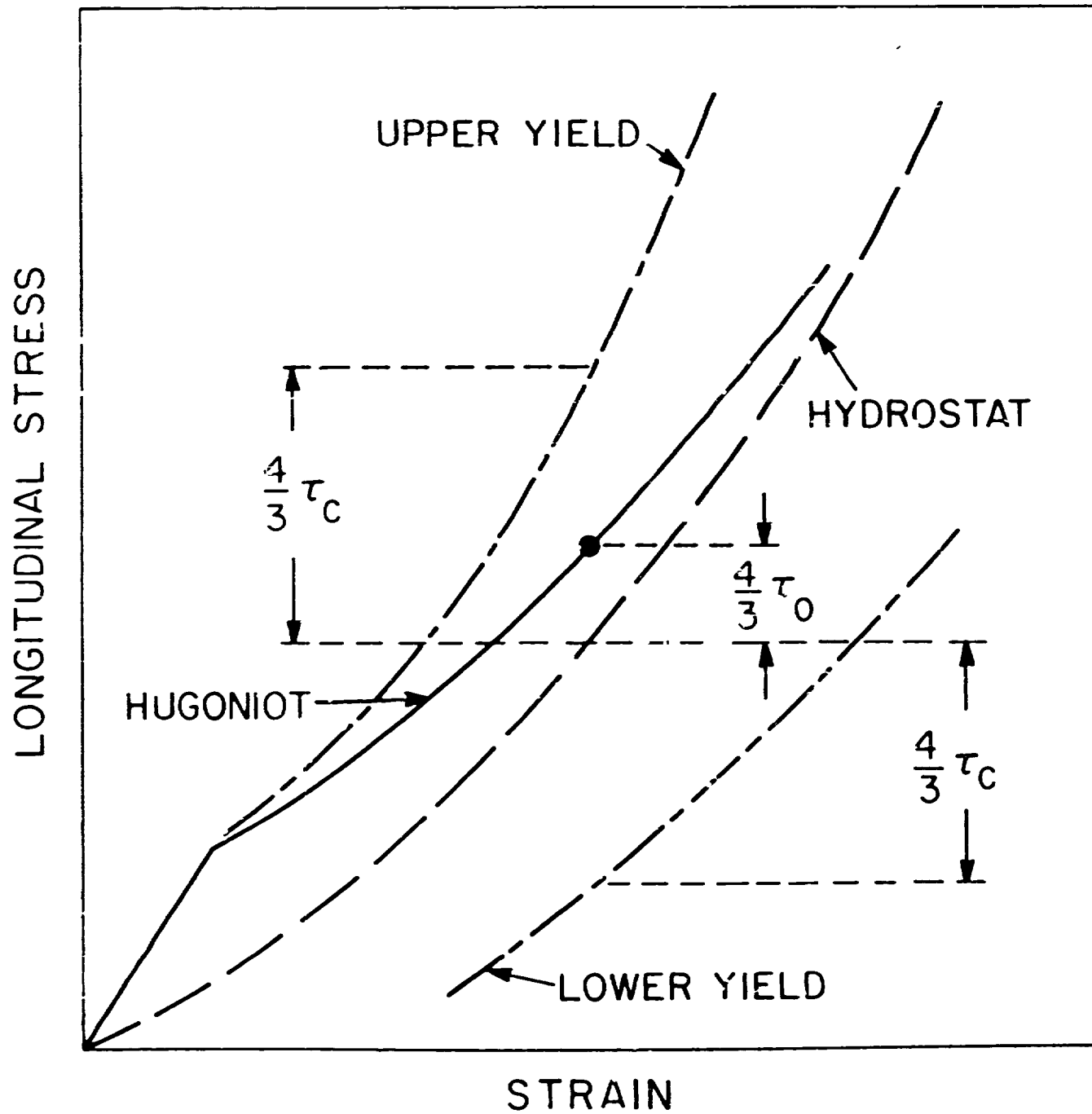


Figure 2.

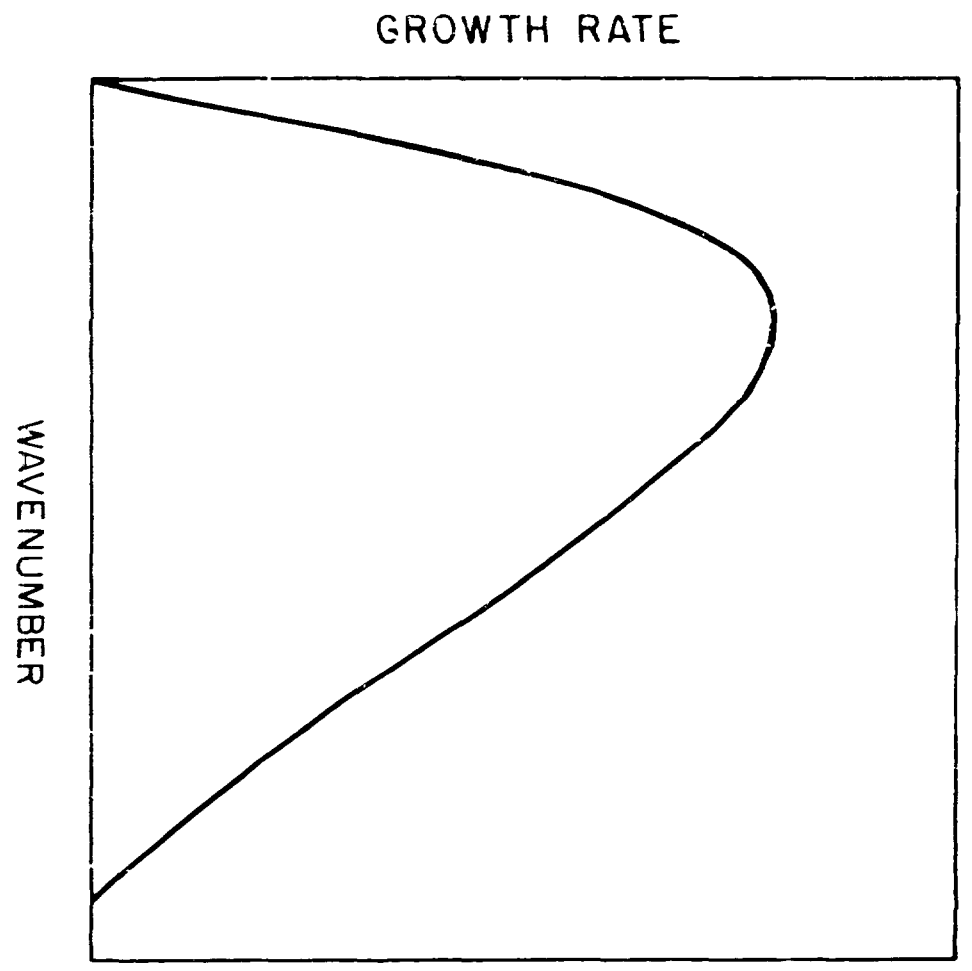


Figure 3.

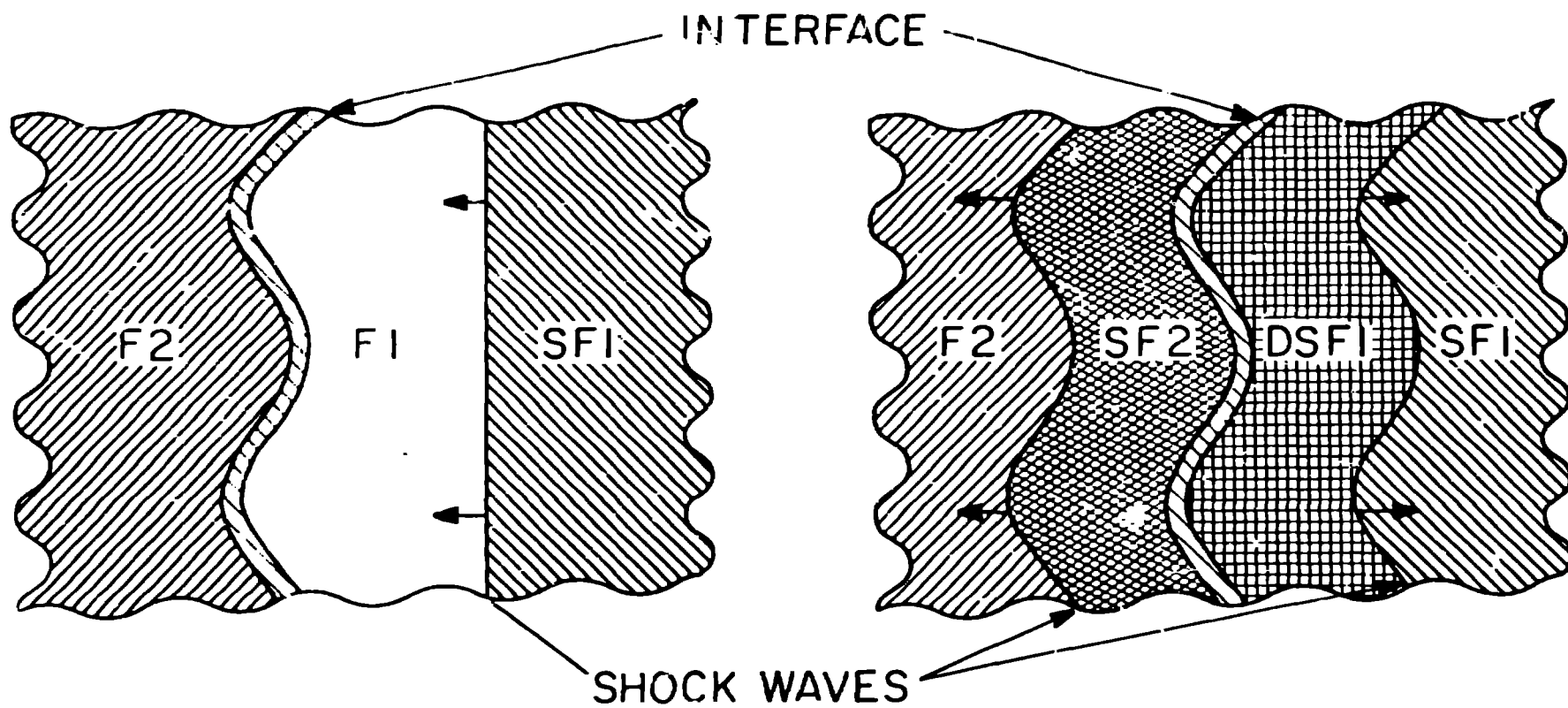


Figure 4.